



ORIGINAL ARTICLE

Cytotoxicity, anti-acute leukemia, and antioxidant properties of gold nanoparticles green-synthesized using *Cannabis sativa* L leaf aqueous extract



Yali Chang^{a,b,*}, Chengyun Zheng^a, Arunachalam Chinnathambi^c,
Tahani Awad Alahmadi^d, Sulaiman Ali Alharbi^c

^a Department of Hematology, The Second Hospital, Cheeloo College of Medicine, Shandong University, No.247, Beiyuan Road, Jinan 250033, PR China

^b Department of Hematology, Jinan Central Hospital, Cheeloo College of Medicine, Shandong University, No.105, Jiefang road, Lixia District, Jinan, Shandong Province 250013, PR China

^c Department of Botany and Microbiology, College of Science, King Saud University, PO Box -2455, Riyadh 11451, Saudi Arabia

^d Department of Pediatrics, College of Medicine, King Saud University, [Medical City], King Khalid University Hospital, PO Box-2925, Riyadh 11461, Saudi Arabia

Received 20 December 2020; accepted 31 January 2021

Available online 11 February 2021

KEYWORDS

Cannabis sativa L;
Gold nanoparticles;
Acute T cell leukemia;
Acute lymphoblastic leukemia;
In vitro condition

Abstract Metallic nanoparticles, especially gold nanoparticles, are used in the therapy of various diseases. Recently, many chemotherapeutic supplements or drugs have been formulated with gold nanoparticles. One option for synthesizing gold nanoparticles is to use herbs. Many previous studies have shown that medicinal herbs increase the antioxidant and cytotoxicity properties of gold nanoparticles against tumor cell lines. In this study, gold nanoparticles were prepared and synthesized in an aqueous medium using *Cannabis sativa* L leaf extract as stabilizing and reducing agents. In addition, we evaluated the anti-leukemia effects of gold nanoparticles against acute T-cell leukemia and lymphoblastic leukemia cell lines. Characterization of gold nanoparticles was done with FE-SEM, FT-IR, UV-Vis and TEM. The MTT test is used for anti-HAuCl₄, *C. sativa* and *C. sativa* aqueous extract and gold nanoparticles, the DPPH test was used in the presence of butylated hydroxytoluene as control. In UV-Vis, the clear peak at 538 nm wavelength showed the formation of gold nanoparticles. In the FT-IR, many antioxidant molecules with relevant bonds led to the perfect condition for gold reduction in gold nanoparticles. In addition, in TEM and FE-SEM images, gold nanopar-

* Corresponding author at: Department of Hematology, The Second Hospital, Cheeloo College of Medicine, Shandong University, No.247, Beiyuan Road, Jinan 250033, PR China.

E-mail address: doctorchangyali@sina.com (Y. Chang).

Peer review under responsibility of King Saud University.



ticles were spherical, with an average size of 18.6 nm. The IC₅₀ of gold nanoparticles were 329, 381, 275 and 218 µg / mL against MOLT-3, TALL-104, J.RT3-T3.5 and Clone E6-1 cell lines, and Jurkat, respectively. The best results of the anti-acute leukemia properties of gold nanoparticles were obtained in the Clone E6-1 cell line. Gold nanoparticles inhibited half of the DPPH at a concentration of 196 µg/mL. The above results confirm the excellent roles of the gold nanoparticles as new chemotherapeutic drugs in treating various types of acute leukemia.

© 2021 Published by Elsevier B.V. on behalf of King Saud University. This is an open access article under the CC BY-NC-ND license (<http://creativecommons.org/licenses/by-nc-nd/4.0/>).

1. Introduction

Traditional medicine (also known as indigenous or folk medicine) comprises medical aspects of traditional knowledge that developed over generations within various societies before modern medicine (Zangeneh and Zangeneh, 2019; Zangeneh, 2019; Mohammadi et al., 2019). Examples of folk medicine traditions are traditional Chinese medicine, traditional Korean medicine, Arabic indigenous medicine, Uyghur traditional medicine, Japanese Kampō medicine, traditional Aboriginal bush medicine, and Georgian folk medicine. Herbal medicines include herbs, herbal materials, herbal preparations and finished herbal products that contain as active ingredients parts of plants, or other plant materials, or combinations (Mahdavi et al., 2019; Tahvilian et al., 2019; Ahmeda et al., 2020). The prevalence of folk medicine in certain areas of the world varies according to cultural norms. Some modern medicine is based on plant phytochemicals that had been used in folk medicine. Researchers state that many of the alternative treatments are “statistically indistinguishable from placebo treatments” (Ghaneialvar et al., 2019; Goorani et al., 2019; Jalalvand et al., 2019; Moradi et al., 2019). One of the plants in traditional medicine is *Cannabis sativa* L from *Rosales* order, *Cannabaceae* family, and *Cannabis* genus. Many species exist in this genus, but *Cannabis indica*, *Cannabis sativa*, and *Cannabis ruderalis* are the most important due to their therapeutic potentials. Among all species from the *Cannabis* genus, *Cannabis sativa* L has a role place (Rashidi et al., 2018; Sherkatolabbasieh et al., 2017; Zhaleh et al., 2018). *C. sativa* has long been administrated for hemp seeds, hemp fiber and their essential oils and oils, hemp leaves for use as juice and as vegetables, medicinal aims, and as a recreational drug (Lozano, 2001). It has been used as a psychoactive drug, as a folk medicine ingredient, and as a source of textile fiber since ancient times. It contains 421 substances of 18 chemical types—the most significant compound is δ9-tetrahydrocannabinol, which causes several effects, both in the Central Nervous System and in several peripheral locations in the organism (Chandra et al., 2010; Gagne et al., 2012). The main antioxidant components of *C. sativa* are linoleic acid, α-linolenic acid, stearidonic acid, oleic acid, palmiticstearic acid, and γ-tocopherol (Wolach, 2015). In medicine, *C. sativa* is used for its antioxidant, anti-inflammatory, antiemetic, anti-parasitic, antibacterial, antiviral, antifungal, antipyretic, pain-killing, cutaneous wound healing, carminative, diuretic, anti-abscesses, anticancer, antiepileptic, anti-anemic, hepatoprotective, nephroprotective, immunoprotective, hematoprotective, splenoprotective, and gastroprotective properties. In medicine, people use *C. sativa* for therapy of blood disorders

like iron deficiency, hematotoxicity, thrombocytopenia, anemia, and especially leukemia (Boer and Boer, 2017).

Leukemia is a common kind of cancer that is caused in the blood. People of both developing and developed countries suffer from this cancer. The frequency and deaths of patients of leukemia were 2,300,000 new cases and 353000, respectively, in 2015. Leukemia occurs more in people in the range ages 55–86 years old (Brown, 2013). This cancer is divided to two parts; acute leukemia and chronic leukemia. The clinical sign and severity of acute leukemia are more (Abdel-Fattah and Ali, 2018). The main risk factors of acute leukemia are genetic factors, family history, environmental pollutants, host susceptibility, certain chemicals, smoking, impaired immune system, and prior radiation therapy. The main symptoms of acute leukemia are cyanosis, the appearance of blood in the feces or urine, bone pain, swollen lymph nodes, mild fever, bleeding and swollen gums, consistent and severe bleeding, and anemia along with paleness and fatigue. Usually for the diagnosis of this type of leukemia, blood test and bone marrow biopsy are used. Other diagnostic tests are imaging, sonography, and physical examination (Zhaleh et al., 2019). In severe situations, immunotherapy, chemotherapy, radiation therapy, and surgery are administrated for the treatment of acute leukemia (Paciotti et al., 2004). The chemotherapeutic drugs have many side effects, so finding a new drug with the efficacy of the chemotherapeutic drugs and without any side effect is very valuable. In this regard, many studies have proven the excellent anticancer properties of metallic nanoparticles containing natural compounds (Paciotti et al., 2006).

Recently, metal-based nanoparticles with distinctive physicochemical properties are recognized as a promising alternative medicine for treating various diseases (Abdel-Fattah and Ali, 2018). Previously, gold was used as a therapeutic factor. Gold nanoparticles are of great interest due to their low cost, availability and known healing activity (Zhaleh et al., 2019). Among all nanoparticles, gold nanoparticles have received rigorous attention due to their wide application in optical, electrical, chemical, sensor, bioremediation, and biochemical fields (Paciotti et al., 2004). Researchers from Maryland gold nanoparticles used a colloidal gold vector to deliver the TNF to solid tumors in mice (Paciotti et al., 2006). Upon intravenous injection, gold nanoparticles conjugated with TNF rapidly accumulates in tumor cells and is not detected in cells of the liver, spleen, and other healthy organs. Accumulation of gold nanoparticles in the tumor is attested by the change in the tumor color; the tumor acquires a bright red/purple color (the color typical of colloidal gold and its aggregates), which coincides with the maximum of tumor-specific activity of the TNF. The colloidal gold–TNF vector had lower toxicity and higher

efficacy in reducing tumor size than the native TNF, since the maximum antitumor reaction was attained by using lower doses of the drug. The preparation for intravenous administration based on a gold nanoparticles–TNF conjugate named AurImmune™ has already passed the second stage of clinical trials (Paciotti et al., 2004 and 2006).

Gold nanoparticles synthesized by plants have been used extensively in biomedical sciences in the therapy of many diseases. Due to the low cost and high availability of medicinal plants, the green synthesis of gold nanoparticles by medicinal plants has increased significantly (Boer and Boer, 2017). Remarkable applications of gold nanoparticles synthesized green every year are gained and this trend continues. Recently synthesized by plants, gold nanoparticles have been formulated for their anti-cancer, anti-inflammatory, wound-healing, antioxidant, antiviral, antifungal, anti-parasitic and antibacterial properties (Abdel-Fattah and Ali, 2018). The results of plenty of studies have indicated important antibacterial properties of gold nanoparticles green-synthesized by plant cells in the treatment of *Bacillus*, *Pseudomonas*, *Streptococcus*, *Salmonella*, and *Staphylococcus* infectious and their antifungal effects in treating candida diseases (Zhaleh et al., 2019). The main therapeutic potentials of gold nanoparticles are anticancer effects. Many previous researches have indicated excellent anticancer properties of gold nanoparticles against common cancer cell lines such as MCF-7/ADR breast cancer, RKO, HCT15, HCT116, and HT29 colon cancer, and LN229, A549, C0045C, Vero, U87, HDF, HepG2-R, and HeLa human glioma cell lines (Paciotti et al., 2004 and 2006). So far, no study hasn't been done about the remedial capacities of gold nanoparticles containing natural compounds in the therapy of acute leukemia.

Based on our knowledge, comparative research on the anti-acute leukemia potentials of HAuCl₄, *C. sativa* leaf, and gold nanoparticles synthesized by *C. sativa* leaf (AuNPs) against acute leukemia cell lines. So, the goal of the present experiment was to investigate the properties of HAuCl₄, *C. sativa* leaf, and AuNPs against acute lymphoblastic leukemia and T cell.

2. Material and methods

2.1. Material

All materials were obtained from Sigma Aldrich chemicals.

3. Preparation and extraction of *C. Sativa*

In this work, after detecting *C. sativa*, it was collected at an altitude of 1400 m above sea level in the spring of 2019. The fresh collected *C. sativa* leaf was dried in the shade for 14 days at room temperature.

Extraction was performed by dissolving 100 g of *C. sativa* leaf powder in 1000 mL of distilled water and keeping in an orbital shaker for 48 h. In addition, herbal extracts were lyophilized for 24 h at -48°C and stored for later use (Paciotti et al., 2004).

4. Synthesis of AuNPs

Synthesis of gold nanoparticles was initiated by the reaction mixture of 100 mL of HAuCl₄·H₂O at a concentration of

1 mM and 10 mL of *C. sativa* leaf aqueous extract (20 μg / mL) in a flask. The mixture was centrifuged at 10000 rpm for 15 min. The precipitate was washed triple with water and then centrifuged (Paciotti et al., 2004). The morphological properties of AuNPs in terms of shape and size were analyzed by FE-SEM and TEM microscopic techniques. Also, AuNPs were first verified using UV–Vis spectroscopy in a scanning range from 100 to 700 nm wavelength (Jasco V670 Spectrophotometer).

5. Determination of the antioxidant impact of AuNPs by DPPH

The DPPH method is a common method for assessing the antioxidant activity of plant species and metallic nanoparticles. It is based on trapping the free radicals of the material, called DPPH, using antioxidant agents that reduce the absorption rate at 517 nm wavelength. When the DPPH solution is mixed with a material that can donate hydrogen atom, radical resuscitation is formed, followed by color reduction. This reaction eliminates the purple color, whose index is forming an absorption band at 517 nm (Zhaleh et al., 2019).

To determine the radical scavenging activity of the HAuCl₄, *C. sativa* and AuNPs, 1 mL of 50 μM DPPH was combined with 1 mL of variable concentrations (0–1000 μg/mL) of HAuCl₄, *C. sativa* and AuNPs. Then, they were transferred to the 37 °C for 1 h. The samples absorption rate was determined at 517 nm by a spectrophotometer, and the antioxidant activity was calculated by the below formula (Zhaleh et al., 2019):

$$\%Inhibition = [A_{blank} - A_{sample} / A_{blank}] \times 100$$

The blank sample contained 1 mL methanol and 1 mL HAuCl₄, *C. sativa* and AuNPs, and a sample of 1 mL DPPH (Zhaleh et al., 2019).

Calculation of half-maximal inhibitory concentration (IC₅₀) is a suitable method for comparing the activity of pharmaceutical materials. In this method, the measurement and comparison criterion is the concentration in which 50% of the final activity of the drug occurs. In this experiment, the IC₅₀ of various repeats is estimated and compared with the IC₅₀ of BHT, which is introduced as the antioxidant activity index. The closer is the obtained value to the IC₅₀ of BHT, the stronger is the antioxidant activity of the material. The graph of the IC₅₀ of the extract was produced by drawing the percent inhibition curve versus the extract concentration. First, three stock samples with variable concentrations (0–1000 μg/mL) of HAuCl₄, *C. sativa* and AuNPs were prepared. Then, a serial dilution was prepared from each sample, and IC₅₀ of the above samples was measured separately, following which their mean was calculated. BHT, with different concentrations, was considered positive control. All experiments were performed in triplicate (Zhaleh et al., 2019).

6. Measurement of cell toxicity and anti-acute leukemia potentials of AuNPs

In this part, HUVEC (Normal cell line), MOLT-3 (Acute lymphoblastic leukemia cell line), TALL-104 (Acute lymphoblastic leukemia cell line), and J .RT3 -T3.5 was prepared to investigate the anticancer effects of HAuCl₄, *C. sativa* and AuNPs using an MTT assay.

They were then cultured as a monolayer culture in 90% RPMI-1640 medium and 10% fetal serum and supplemented with 200 mg/mL streptomycin, 125 mg/mL penicillin, and 8 mg/mL amphotericin B. The culture was then exposed to 0.5 atmospheric carbon dioxide at 37 °C, on which the tests were performed after at least ten successful passages. MTT assay a method used to investigate the toxic effects of various materials on various cell lines, including non-cancer and cancer cells. To evaluate the cell toxicity effects of the compounds used in this research, the cells were transferred from the T25 flask to the 96-well flasks. In each cell of the 96-cell flasks, 7000 cells of cancer and fibroblast cell lines were cultured, and the volume of each cell was eventually increased to 100 μ L. Before the treatment of the cells in the 96-well flask, the density of cells was increased to 70%, so the 96-well flasks were incubated for 24 h to obtain the cell density of 7×10^3 . Next, the initial culture medium was discarded, and variable concentrations (0–1000 μ g/mL) of HAuCl₄, *C. sativa* and AuNPs were incubated at 37 °C and 0.5 CO₂ for 24, 48, and 72 h. Then, 20 μ L MTT was added to each well after a certain amount of time. Next, 100 μ L DMSO solvent was added to each well. They were then kept at room temperature for 25 min and read at 490 and 630 nm by a microtitre plate reader (Sanchez-Moreno et al., 1998; Arulmozhi et al., 2013).

The cell lines were treated with the hydroalcoholic extract (1.25 mg/mL), which inhibited about 20% of the cell growth. Annexin/PI method was used to determine the apoptosis level in the treated and control cell lines using a flow cytometry machine. To the experiment, the cell lines were treated with a variable concentration (0–1000 μ g/mL) of HAuCl₄, *C. sativa* and AuNPs for 24 h. Cells were irrigated with phosphate-buffered saline (PBS). After centrifugation, buffer binding was added to the obtained precipitate. Then, 5 μ L Annexin V dye was added and incubated for 15 min at 25 °C. Cells were washed with the binding solution, following which 10 μ L PI dye was added. Finally, cell analysis was done by a flow cytometry machine according to the below formula (Arulmozhi et al., 2013):

$$\text{Cell viability(\%)} = \frac{\text{Sample A.}}{\text{Control A.}} \times 100$$

The closer is the obtained value to the IC₅₀ of HAuCl₄, *C. sativa* and AuNPs, the stronger is the cell viability activity of the material. The graph of the IC₅₀ of the extract was produced by drawing the percent inhibition curve versus the extract concentration. First, three stock samples with variable concentrations (0–1000 μ g/mL) of HAuCl₄, *C. sativa* and AuNPs were prepared. Then, a serial dilution was prepared from each sample, and IC₅₀ of the above samples was measured separately, following which their mean was calculated.

6.1. Statistical analysis

Data related to absorbance measurements were entered into the Microsoft® Excel and then transferred to Minitab statistical. This was recorded to fit the parametric data assumptions and expressed as Means \pm Standard Deviation (SD). The results data are recorded in Figures.

7. Results and discussions

7.1. Chemical characterization of AuNPs

UV-Vis. The spectra of AuNPs biosynthesized using the *C. sativa* leaf aqueous extract are shown in Fig. 1. Optical properties derived from UV-Vis. A peak at 538 nm belongs to synthetic AuNPs. This observation is in good agreement with previous works on the biosynthesis of AuNPs nanoparticles (Oganesvan et al., 1991).

To record TEM images, drop-coated films of AuNPs obtained by the reaction of *C. sativa* leaf aqueous extract with HAuCl₄ were used. Fig. 2 shows the shape and size it. The resulting AuNPs were found spherical and mean size 18.6 nm. In rare cases, larger-sized particles were also observed in the sample, but their numbers were rather low. The rapid reduction of gold ions with the aqueous extract of *C. sativa* leaf resulted in homogeneous nucleation of gold metals, resulting in forming small size AuNPs. AuNPs are trapped in a *C. sativa* matrix composed of biomolecules, possibly acting as a capping or stabilizing agent during synthesis.

Fig. 3 shows a successful synthesis of gold nanoparticles with spherical morphology. The pictures also confirm that biosynthesized AuNPs are uniform, well dispersed and homogeneous. A tendency for aggregation is also observed for synthetic nanoparticles. This property of metallic nanoparticles synthesized using environmentally friendly methods such as FeNPs, CdNPs, AuNPs, AgNPs, CuNPs, and TiNPs has been previously reported (Tian et al., 2010; Harshiny et al., 2015; Ghidan et al., 2016). Particle size for AuNPs averaged 18.6 nm in diameter.

In our literature review, different sizes among 10–50 nm have been recorded for AuNPs biosynthesized using plant extracts by TEM and FE-SEM (Rao and Pennathur, 2017).

The secondary metabolites responsible for the reduction and restriction of the HAuCl₄ precursor to AuNPs were investigated using the FT-IR technique. Presence of different IR bands related to various functional groups in *C. sativa* leaf aqueous extract. For example, peaks at 3442 and 2917 cm⁻¹ are related to O-H and aliphatic C-H stretch; Peaks in the

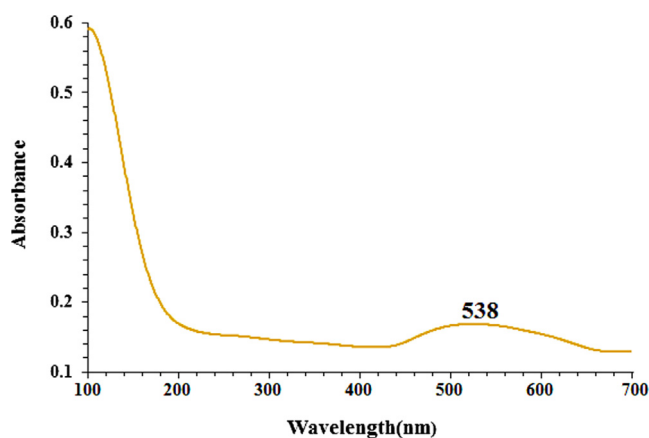


Fig. 1 The UV-Vis spectrum of biosynthesized AuNPs.

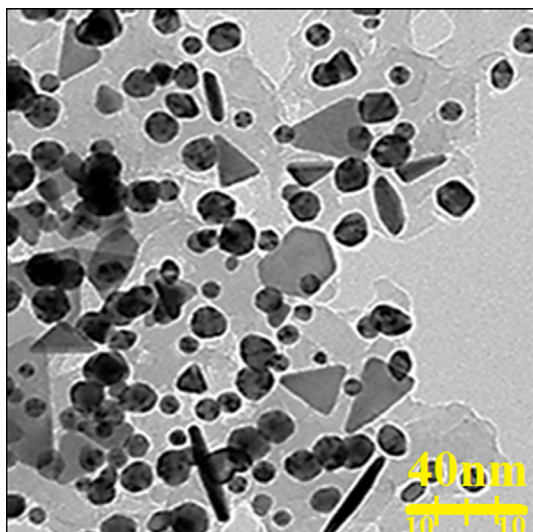


Fig. 2 TEM image of AuNPs.

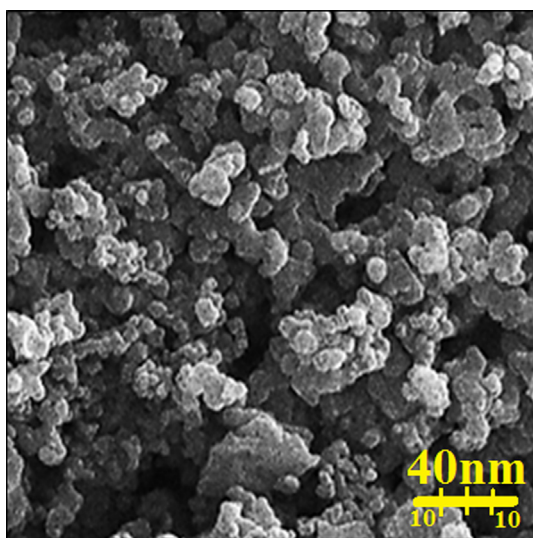


Fig. 3 FE-SEM image of AuNPs.

range of 1628 to 1765 cm^{-1} correspond to $\text{C}=\text{C}$ and $\text{C}=\text{O}$ stretch, and peaks at 1100 and 1029 cm^{-1} can be attributed to $-\text{C}-\text{O}$ and $-\text{C}-\text{O}-\text{C}$ stretch (Fig. 4). The peaks at the wavenumbers of 434 and 542 cm^{-1} refer to the $\text{Au}-\text{O}$. These peaks can be recorded for the presence of diverse molecules like flavonoid, phenolic, and carboxylic molecules previously reported (Baghayeri et al., 2018; Seydi et al., 2019).

8. Cytotoxicity activity of AuNPs

In the present study, treated cells with different concentrations of HAuCl_4 , *C. sativa* and AuNPs were examined by 48-hour MTT test for cytotoxicity effect on the HUVEC (Normal cell line), MOLT-3 (Acute lymphoblastic leukemia cell line. –104 (Acute lymphoblastic leukemia cell line) (Figs. 5-7). The absorbance rate was determined at 570 nm and this showed exceptional viability for HAuCl_4 , *C. sativa* and AuNPs even up to

$1000\text{ }\mu\text{g} / \text{mL}$ in the normal cell line (HUVEC). HAuCl_4 , *C. sativa* and AuNPs do not have any significant toxicity has many safe applications in biochemical and medical fields.

In the case of acute lymphoblastic leukemia cell lines (MOLT-3 and TALL-104) their viability decreased in a dose-dependent manner in the presence of HAuCl_4 , *C. sativa* and AuNPs. The IC_{50} of *C. sativa* and AuNPs against the MOLT-3 cell line were 535 and $329\text{ }\mu\text{g} / \text{mL}$, respectively, and 673 and $381\text{ }\mu\text{g} / \text{mL}$ against the TALL-104 cell line, respectively. In the case of acute T cell leukemia cell lines (Jurkat, Clone E6-1 and J.RT3-T3.5) their viability decreased in a dose-dependent manner in the presence of HAuCl_4 , *C. sativa* and AuNPs. The IC_{50} of *C. sativa* and AuNPs against Jurkat, Clone E6-1 cell lines were 218 and $502\text{ }\mu\text{g} / \text{mL}$, respectively, and 275 and $567\text{ }\mu\text{g} / \text{mL}$ against the J.RT3-T3.5 cell line, respectively. The best result was seen in the case of the Jurkat, Clone E6-1 cell line.

About potential of gold nanoparticles, they have used it in the treatment of various cancers such as human glioma, colon cancer, lung epithelial cancer, Lewis lung carcinoma, breast carcinoma, uterine cancer and human lung cancer (Dou et al., 2020). It was found that the anticancer of gold nanoparticles is highly dependent on a number of factors related to its physical properties such as shape, surface coverage, and size. About size, it has been stated that small-sized gold nanoparticles can transfer and remove the cell membrane of tumor cells. In the larger size, the above capability is significantly limited (Namvar et al., 2014). As shown in Figs. 3 and 4 of our study, gold nanoparticles had a uniform spherical morphology of 18.6 nm in size. The size of gold nanoparticles below 50 nm is well suited for killing tumor cell lines in vivo and in vitro (Namvar et al., 2014).

Regarding the anticancer properties of *C. sativa*, it has been reported that cell proliferation is reduced in colorectal cancer cell lines following treatment with *C. sativa*. Safaraz et al. (2008) (Safaraz et al., 2008), Chen et al. (2011) (Chen et al., 2011), and Sharma et al. (2014) (Sharma et al., 2014) Cannabidiol-rich *C. sativa* extracts were able to induce cell death in prostate cancer cell lines PC3, DU145, and LNCaP at low doses ($20\text{--}70\text{ }\mu\text{g} / \text{ml}$). Sharma et al. (2014) pointed to a similar cell death pattern, so treatment of prostate cancer cell lines with *C. sativa* resulted in induction of apoptosis (Sharma et al., 2014). About the cytotoxicity mechanism of this strain, *C. sativa* is involved in the induction of apoptosis via the death receptor pathway, by binding to the Fas receptor, or by Bax activation induced by ceramide synthesis in cells. However, little has been revealed about the induction of apoptosis by *C. sativa* through activation of p53 (Bla'zquez et al., 2000).

9. Antioxidant effect of AuNPs

In the present study, the *C. sativa* aqueous extract and BHT-like AuNPs showed an important concentration-dependent DPPH radical scavenging property. Interaction between *C. sativa* leaf extract and AuNPs and DPPH (Kalita et al., 2013; Kedare and Singh, 2011; Matthaus, 2002). The IC_{50} values of *C. sativa* extract, BHT, and AuNPs were 361 , 324 , and 196 , respectively (Fig. 8). The antioxidant property exhibited by *C. sativa* can be attributed to the presence of several phytochemicals thought to act interactively and synergistically to neutralize free radicals. In the previous study, *C. sativa* was

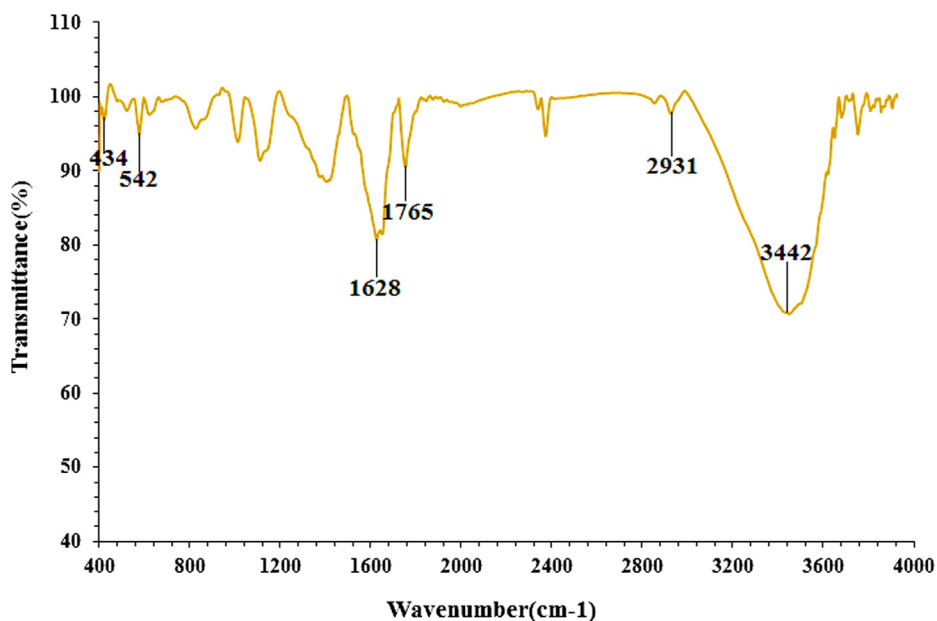


Fig. 4 FT-IR spectra of biosynthesized AuNPs.

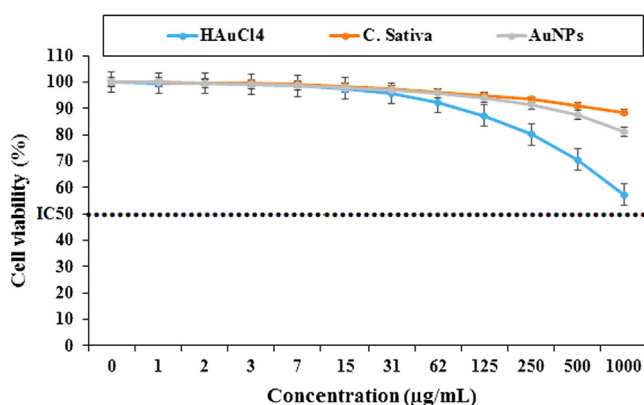


Fig. 5 Percent viability measured on HUVEC after treatment with present HAuCl₄, *C. sativa*, and AuNPs.

reported to be rich in antioxidant compounds such as γ -tocopherol, palmiticstearic acid, oleic acid, stearidonic acid, α -linolenic acid, and linoleic acid. These bioactive molecules have been recorded to maintain redox homeostasis through multi-step antioxidant reaction processes that involve propagation, branching, initiation, and termination of free radicals (Aliev et al., 2009; Ishino et al., 2010).

Previous research has also demonstrated DPPH activities of diverse plant extracts. Flower, Leaf, and stem extracts of *Thymelaea hirsuta* showed a concentration-dependent activity on DPPH assay (Amari et al., 2014). Methanolic whole plant extract of *Biophytum sensitivum* determined anti-radical activity with a maximum inhibition of about 43.96% in scavenging DPPH radical.

According to our research, there is the only research on the antioxidant activity of *C. sativa*. Nafis et al. (2019), (Nafis et al., 2019) IC₅₀ values of 1.8 ± 0.2 mg / mL for *C. sativa*-carotene / linoleic acid test, 0.9 ± 0.1 mg / mL and free DPPH for power reduction (Nafis et al., 2019).

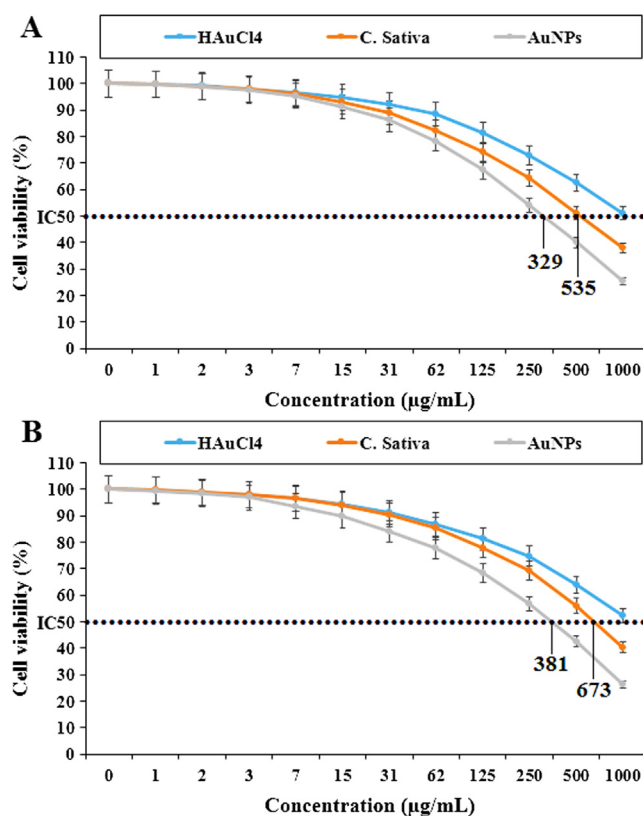


Fig. 6 Percent viability measured on acute lymphoblastic leukemia cell lines including MOLT-3 (A) and TALL-104 (B) after treatment with present HAuCl₄, *C. sativa*, and AuNPs.

The important anti-acute leukemia potentials of gold nanoparticles synthesized with the aqueous extract of *C. sativa* against acute T cell leukemia and acute lymphoblastic leukemia cell lines are correlated with their antioxidant activities.

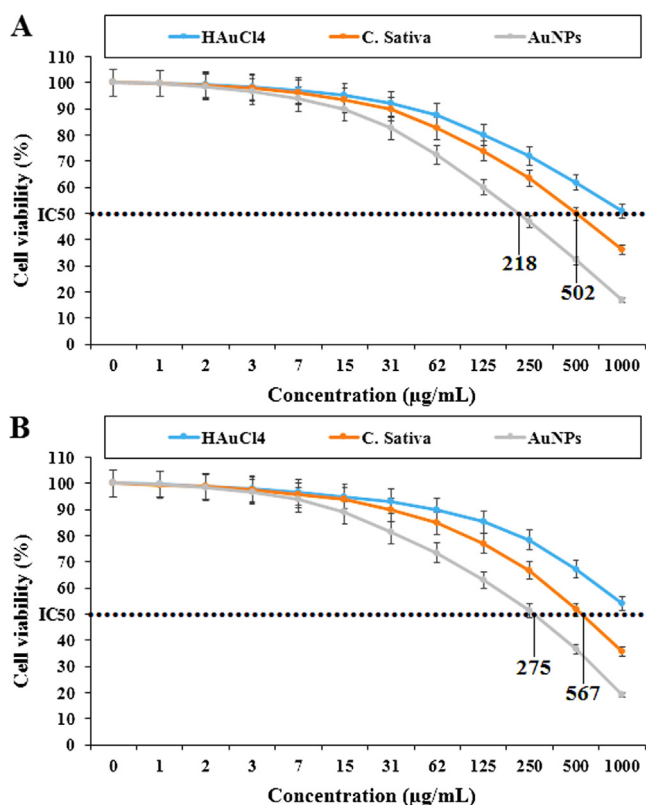


Fig. 7 Percent viability measured on acute T cell leukemia cell lines including Jurkat, Clone E6-1 (A) and J.RT3-T3.5 (B) after treatment with present HAuCl₄, *C. sativa*, and AuNPs.

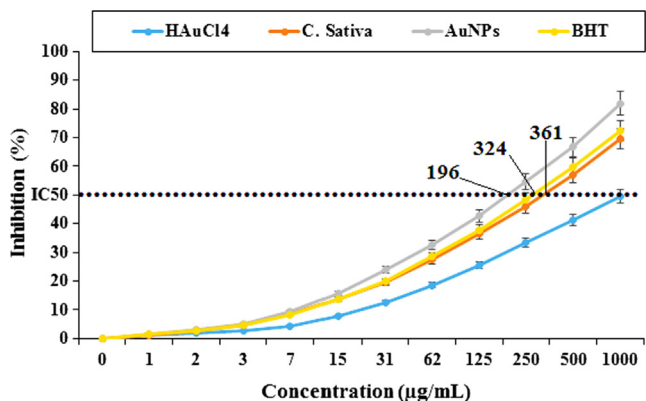


Fig. 8 Antioxidant potential of HAuCl₄, *C. sativa*, AuNPs, and BHT. BHT: Butylated hydroxyl toluene.

Similar studies have revealed that antioxidant molecules like metallic nanoparticles, especially gold nanoparticles and ethnomedicinal plants, reduce the volume of tumors by eliminating free radicals. (Katata-Seru et al., 2018; Sangami et al., 2017) In detail, the high presence of free radicals in normal cells causes many mutations, destroying gene expression in DNA and RNA and then accelerating the proliferation and growth of abnormal cells or cancerous cells (Beheshtkhoo et al., 2018) High availability in all cancers such as breast, free radicals, stomach, gall bladder, liver, rectal, gastrointestinal stromal, bile duct, esophagus, small intestine, pancreas, colon,

thyroid, parathyroid, prostate, bladder, testicle, vaginal, fallopian tube, ovarian, throat, lung, hypo pharyngeal, and skin cancers show the important role of these molecules in making angiogenesis, and (Radini et al., 2018) Many researchers reported that gold nanoparticles synthesized by ethno medicinal plants have a remarkable role in the removal of free radicals (Beheshtkhoo et al., 2018; Radini et al., 2018).

10. Conclusion

Gold nanoparticles were successfully determined from bio-reduction of HAuCl₄ solutions using an aqueous extract of *C. sativa* leaf. AuNPs have been characterized and validated using TEM, FE-SEM, UV-Vis and FT-IR. Gold nanoparticles showed favorable antioxidant and anticancer activities towards acute lymphoblastic leukemia and acute T without any cytotoxic effect on the normal cell line. Gold nanoparticles synthesized using the aqueous extract of *C. sativa* leaf can be used for the therapy of acute lymphoblastic leukemia and acute T cell leukemia in humans after being approved in vivo experiments and clinical trials.

Funding

This work was supported in part by research funding from the National Natural Science Foundation of China (81372545), Business Plan Foundation of Jinan for the Scholar to Study Abroad (20100206), The funders had no role in the study design, data collection and analysis, decision to publish, or preparation of the manuscript.

Declaration of Competing Interest

The authors declared that there is no conflict of interest.

Acknowledgement

This project also was supported by Researchers Supporting Project number (RSP-2020/230) King Saud University, Riyadh, Saudi Arabia.

Data availability statement

Data available on request due to privacy/ethical restrictions (The data that support the findings of this study are available on request from the corresponding author. The data are not publicly available due to privacy or ethical restrictions).

References

- Zangeneh, A., Zangeneh, M.M., Moradi, R., 2019a. Appl Organometal Chem. 33. <https://doi.org/10.1002/aoc.5247>. e5247.
- Zangeneh, A., Zangeneh, M.M., 2019. Appl Organometal Chem. 33. <https://doi.org/10.1002/aoc.5290>. e5290.
- Abdel-Fattah, W.I., Ali, G.W., 2018. J Appl Biotechnol Bioeng. 5, 00116.
- Ahmeda, A., Zangeneh, A., Zangeneh, M.M., 2020. Appl Organometal Chem 34. <https://doi.org/10.1002/aoc.5290>. e5290.
- Aliev, G. et al, 2009. Neurotox. Res. 16, 293–305.
- Amari, N.O., Bouzouina, M., Berkani, A., Lotmani, B., 2014. Phytochemical screening and antioxidant capacity of the aerial parts of *Thymelaea hirsuta* L. Asian Pac J Trop Dis 4 (2), 104–109.
- Arulmozhi, V., Pandian, K., Mirunalini, S., 2013. Ellagic acid encapsulated chitosan nanoparticles for drug delivery system in human oral cancer cell line (KB). Colloids Surf B Biointerfaces 110, 313–320.

- Mahdavi, B., Paydarfard, S., Zangeneh, M.M., Goorani, S., Seydi, N., Zangeneh, A., 2019. *Appl Organometal Chem.* 33. <https://doi.org/10.1002/aoc.5248>. e5248.
- Baghayeri, M., Mahdavi, B., Hosseinpor-Mohsen Abadi, Z., Farhadi, S., 2018. Green synthesis of silver nanoparticles using water extract of *Salvia leriifolia*: Antibacterial studies and applications as catalysts in the electrochemical detection of nitrite. *Appl Organometal Chem.* 32 (2). <https://doi.org/10.1002/aoc.v32.210.1002/aoc.4057>.
- Beheshtkhou, N., Kouhbanani, M.A.J., Savardashtaki, A., Amani, A. M., Taghizadeh, S., 2018. Green synthesis of iron oxide nanoparticles by aqueous leaf extract of *Daphne mezereum* as a novel dye removing material. *Appl. Phys. A* 124 (5). <https://doi.org/s00339-018-1782-3>. *FASEB J.* 14, 2315–2322.
- Boer, J.M., den Boer, M.L., 2017. *Eur. J. Cancer* 82, 203–218.
- Brown, P., 2013. *Hematology. American Society of Hematology. Education Program.* 1, 596–600.
- Chandra, S., Lata, H., Khan, I.A., ElSohly, M.A., 2010. *Medicinal Plant Biotechnology.* Arora, USA, pp. 98–114.
- Chen, P. et al, 2011. *Anticancer Drugs Preclinical Rep.* 23, 437–444.
- Dou, L., Zhang, X., Zangeneh, M.M., Zhang, Y., 2020. Efficient biogenesis of Cu₂O nanoparticles using extract of *Camellia sinensis* leaf: Evaluation of catalytic, cytotoxicity, antioxidant, and anti-human ovarian cancer properties. *Bioorg. Chem.* 106, 104468.
- Mohammadi, G., Zangeneh, M.M., Zangeneh, A., Siavosh Haghighi, Z.M., 2019. *Appl Organometal Chem.* 33. <https://doi.org/10.1002/aoc.5136>. e5136.
- Gagne SJ, Stout JM, Liu E, Boubakir Z, Clarck SM, Page JE. *Proc Natl Acad Sci USA.* 2012;109:12811-6. (d) Pertwee RG. *Br J Pharmacol.* 2006 Jan;147:163-1.
- Ghaneialvar, H., Sahebghadam Lotfi, A., Arjmand, S., et al, 2019. *Comp Clin Path.* 28, 1077–1085.
- Ghidan, A.Y. et al, 2016. *Environ Nanotechnol Monitor Manag.* 6, 95–98.
- Goorani, S., Koochi, M.K., Zangeneh, A., et al, 2019. *Comp Clin Path.* 28 (5), 1221–1227.
- Harshiny, M. et al, 2015. *Powder Technol.* 286, 744–749.
- Ishino, K.C. et al, 2010. *J. Biol. Chem.* 285, 15302–15313.
- Jalalvand, A.R., Zhaleh, M., Goorani, S., et al, 2019. *J. Photochem. Photobiol., B* 192, 103–112.
- Kalita, P. et al, 2013. *J Drug Deliv Therap* 3, 33–37.
- Katata-Seru, L. et al, 2018. Green synthesis of iron nanoparticles using *Moringa oleifera* extracts and their applications: Removal of nitrate from water and antibacterial activity against *Escherichia coli*. *J. Mol. Liq.* 256, 296–304.
- Kedare, S.B., Singh, R.P., 2011. Genesis and development of DPPH method of antioxidant assay. *J. Food Sci. Technol.* 48, 412–422.
- Lozano, I., 2001. The Therapeutic Use of *Cannabis sativa* (L.) in Arabic Medicine. *J Cannabis Therap.* 1, 63–70.
- Zangeneh, M.M., 2019. *Appl Organometal Chem.* 33. <https://doi.org/10.1002/aoc.5295>. e5295.
- Matthaus, B., 2002. Antioxidant Activity of Extracts Obtained from Residues of Different Oilseeds. *J. Agric. Food Chem.* 50, 3444–3452.
- Moradi, R., Hajjalani, M., Salmani, S., et al, 2019. *Comp Clin Path.* 28 (5), 1205–1211.
- Nafis, A. et al, 2019. Antioxidant activity and evidence for synergism of *Cannabis sativa* (L.) essential oil with antimicrobial standards. *Ind Crops Prod* 137, 396–400.
- Namvar, F. et al, 2014. Cytotoxic effect of magnetic iron oxide nanoparticles synthesized via seaweed aqueous extract. *Int J Nanomedicine* 19, 2479–2488.
- O. Wolach, R. M. *Blood.* 2015, 125, 2477–2485.
- Oganesvan, G. et al, 1991. Phenolic and flavonoid compounds of *Ziziphora clinopodioides*. *Chem Nat* 27, 247.
- Paciotti, G.F., Kingston, D.G.I., Tamarkin, L., 2006. *Drug Dev. Res.* 67, 47–54.
- Paciotti, G.F., Myer, L., Weinreich, D., Goia, D., Pavel, N., McLaughlin, R.E., Tamarkin, L., 2004. *Drug Deliv.* 11, 169–183.
- Radini, I.A. et al, 2018. Biosynthesis of iron nanoparticles using *Trigonella foenum-graecum* seed extract for photocatalytic methyl orange dye degradation and antibacterial applications. *J. Photochem. Photobiol., B* 183, 154–163.
- Rao, M.D., Pennathur, G., 2017. *Mater. Res. Bull.* 85, 64–73.
- Rashidi, K., Mahmoudi, M., Mohammadi, G., et al, 2018. *Int. J. Biol. Macromol.* 120, 587–595.
- Safaraz, S. et al, 2008. Cannabinoids for cancer treatment: progress and promise. *Cancer Res.* 68, 339–344.
- Sanchez-Moreno, C. et al, 1998. A procedure to measure the antiradical efficiency of polyphenols. *J. Sci. Food Agric.* 76, 270–276.
- Sangami, S. et al, 2017. *Environ Technol Innov* 8, 150–163.
- Seydi, N. et al, 2019. Preparation, characterization, and assessment of cytotoxicity, antioxidant, antibacterial, antifungal, and cutaneous wound healing properties of titanium nanoparticles using aqueous extract of *Ziziphora clinopodioides* Lam leaves. *Appl Organometal Chem.* 33. e5009.
- Sharma, M. et al, 2014. In Vitro Anticancer Activity of Plant-Derived Cannabidiol on Prostate Cancer Cell Lines. *Pharmacol Pharm.* 5, 806–820.
- Sherkatolabbasieh, H., Hagh-Nazari, L., Shafiezadeh, S., Goodarzi, N., Zangeneh, M.M., Zangeneh, A., 2017. *Arch. Biol. Sci.* 69 (3), 535–543.
- Tahvilian, R., Zangeneh, M.M., Falahi, H., et al, 2019. *Appl Organometal Chem.* 33. <https://doi.org/10.1002/aoc.5234>. e5234.
- Tian, S. et al, 2010. Determination of oleanolic acid and ursolic acid contents in *Ziziphora clinopodioides* Lam. by HPLC method. *Pharmacog Mag.* 6, 116–119.
- Zhaleh, M. et al, 2019. In vitro and in vivo evaluation of cytotoxicity, antioxidant, antibacterial, antifungal, and cutaneous wound healing properties of gold nanoparticles produced via a green chemistry synthesis using *Gundelia tournefortii* L. as a capping and reducing agent e5015 *Appl Organometal Chem.* 33. <https://doi.org/10.1002/aoc.5015>.
- Zhaleh, M., Sohrabi, N., Zangeneh, M.M., et al, 2018. *J Essent Oil Bear Pl.* 21 (2), 493–501.